

Minimal RB-responsive E1A Promoter Modification to Attain Potency, Selectivity, and Transgene-arming Capacity in Oncolytic Adenoviruses

Juan J Rojas¹, Sonia Guedan¹, Peter F Searle², Jordi Martinez-Quintanilla¹, Raúl Gil-Hoyos¹, Francisca Alcayaga-Miranda¹, Manel Cascallo¹ and Ramon Alemany¹

¹Translational Research Laboratory, IDIBELL-Institut Català d'Oncologia, L'Hospitalet de Llobregat, Barcelona, Spain; ²Cancer Research UK Cancer Centre, University of Birmingham, Birmingham, UK

Oncolytic adenoviruses are promising anticancer agents due to their ability to self-amplify at the tumor mass. However, tumor stroma imposes barriers difficult to overcome by these agents. Transgene expression is a valuable strategy to counteract these limitations and to enhance antitumor activity. For this purpose, the genetic backbone in which the transgene is inserted should be optimized to render transgene expression compatible with the adenovirus replication cycle and to keep genome size within the encapsidation size limit. In order to design a potent and selective oncolytic adenovirus that keeps intact all the viral functions with minimal increase in genome size, we inserted palindromic E2F-binding sites into the endogenous E1A promoter. The insertion of these sites controlling E1A- Δ 24 results in a low systemic toxicity profile in mice. Importantly, the E2F-binding sites also increased the cytotoxicity and the systemic antitumor activity relative to wild-type adenovirus in all cancer models tested. The low toxicity and the increased potency results in improved antitumor efficacy after systemic injection and increased survival of mice carrying tumors. Furthermore, the constrained genome size of this backbone allows an efficient and potent expression of transgenes, indicating that this virus holds promise for overcoming the limitations of oncolytic adenoviral therapy.

Received 5 March 2010; accepted 18 July 2010; published online 31 August 2010. doi:10.1038/mt.2010.173

INTRODUCTION

Despite great advances in the treatment of cancer, it remains one of the leading causes of mortality worldwide. Therefore, research on novel cancer therapies with a high therapeutic index limited to malignant tissues is crucial. Among new treatments proposed to target cancer, oncolytic adenoviruses are a promising and appealing therapy due to their ability to self-amplify selectively at the tumor site.¹ Several oncolytic adenoviruses have already been

tested in clinical trials involving a variety of tumors and routes of administration. Clinical data revealed a good toxicological and safety profile, but some potentially concerning adverse effects were observed after administration at high doses.² With regard to efficacy, most responses detected were transient and the treatment was not able to alter significantly the course of the disease. Overall, this data indicate out a critical need for improved oncolytic potency to result in sustained therapeutic responses in humans.

For an efficient treatment of tumors at an advanced stage, systemic delivery is preferred.³ However, the virus encounters some limitations when injected systemically. First of all, it is quickly eliminated from the bloodstream by the liver or inactivated by binding to blood cells, neutralizing antibodies, or complement,⁴ and only a minimal proportion of the injected dose reaches the tumor. Once in the tumor, the stroma and the antiviral immune response limit the spread of the virus throughout the tumor.⁵ The expression of a therapeutic transgene from the adenoviral backbone is a rational and efficient approach to circumvent these limitations. Armed replicating adenoviruses are a combination of virotherapy and gene therapy strategies in which the input of transgene dose is amplified by replication of the virus and, above all, gene transfer can amplify the antitumor activity of virotherapy. In this regard, several transgenes have been inserted into oncolytic adenoviruses in order to increase cytotoxicity, to stimulate immune responses, or to digest the connective tissue to facilitate intratumoral spread.⁶ However, encapsidation size of the adenovirus type 5 is limited to 105% of the wild-type genome, and larger genomes result in genetic instability and packaging problems.⁷ E3 genes have been deleted to create space for transgenes, but E3 has important immune inhibitory functions that may facilitate virus spread in immunocompetent hosts.⁸ Thus, further research is needed to optimize the transgene expression machinery and the adenoviral backbone in which the transgene is inserted in order to minimize genome size and make transgene expression compatible with both selective and potent replication.

Taking into consideration the concerning adverse effects observed in clinical trials after systemic injection of oncolytic

M.C. and R.A. contributed equally to this work.

Correspondence: Ramon Alemany, IDIBELL-Institut Català d'Oncologia, Av Gran Via de l'Hospitalet, 199–203, L'Hospitalet de Llobregat, 08907 Barcelona, Spain. E-mail: ralemany@iconcologia.net

adenoviruses,² it is important to restrict virus gene expression to tumor cells to ensure virus safety. In mice, *E1A* expression in hepatocytes is enough to cause transaminitis and severe liver injury,⁹ and this toxicity is not prevented by deletions in other viral genes that confer selectivity. Modification of *E1A* transcriptional control is a useful approach to avoid this toxicity. Tissue-specific promoters have been tested in this regard to treat certain types of cancer, such as the *PSA* promoter to target prostate cancer¹⁰ or the *uPAR* promoter for pancreatic tumors.¹¹ However, promoters with a broader tropism are more appealing due to their applicability to different tumor types. Those active in tumors and repressed in normal tissues, such as *E2F-1* (ref. 12) or *hTERT*,¹³ are an ideal option. Nevertheless, some losses of potency with respect to wild-type transcription control were reported when these promoters were placed to control *E1A*, especially when tested in a wide range of cancer models.

In a recent work,¹⁴ we demonstrated that the incorporation of E2F-responsive palindromes in an insulated *E2F-1* promoter controlling E1A- Δ 24 resulted in increased oncolytic potency with a low systemic toxicity profile. The E2F-responsive palindromes boosted a positive feedback loop turned on in cancer cells involving E1A and E4-6/7. However, the combination of genetic elements present in the resulting oncolytic adenovirus (ICOVIR-7) raised its genomic size close to the 105% packaging limit, and this hindered the incorporation of transgenes to this highly tumor-selective backbone. In the present study, we developed a novel oncolytic adenovirus (ICOVIR-15) that achieved selective and potent replication in tumor cells with a genomic size that only exceeds the native Ad5 size by 151 base pairs (bp). Four palindromic E2F-binding sites and one Sp-1-binding site were inserted in the endogenous *E1A* promoter to redirect E1A- Δ 24 transcription toward pRb deregulation. As a consequence, viral replication was enhanced compared to Adwt-RGD in all cancer models tested, and potent antitumor activity was achieved when injected systemically in tumor models *in vivo*. Toxicity caused in mice by Adwt-RGD and Ad Δ 24-RGD was considerably reduced by this modification and allowed safe systemic administration at high doses. Importantly, the reduced genome size of ICOVIR-15 improves its suitability for transgene

expression, and this virus offers considerable promise for cancer gene-virotherapy.

RESULTS

E1A promoter modification

The transcription of the *E1A* gene in wild-type Ad5 is regulated by a variety of cellular and viral protein factors.¹⁵ The transcriptional control region of *E1A* extends from the left terminus of the virus genome to the *E1A* cap site and contains the replication origin of Ad DNA, the inverted terminal repeat, the packaging elements, the transcriptional enhancer elements for the *E1A* gene and other viral early genes, and the promoter proximal elements of the *E1A* gene (Figure 1). ICOVIR-15 is a novel Ad Δ 24-RGD-derivative oncolytic adenovirus that incorporates four E2F-responsive palindromes downstream of the packaging signal to redirect *E1A* transcription toward deregulation of the retinoblastoma (Rb/p16) pathway. These palindromic-binding sites are responsible for the potency and selectivity of the *E2F-1* promoter and play a dual role controlling transcription in response to E2F status.¹⁶ Furthermore, one Sp-1-binding site was also inserted as both transcription factors interact to cooperatively activate transcription.¹⁷ Figure 1 represents schematically the binding sites inserted into the *E1A* promoter and their different role in tumor or normal cells. Importantly, this modification preserves the original structure of the adenovirus genome and the function of the *E1A* enhancer region, which may contribute to an efficient selective replication in the cancer cell without affecting the antitumor potency. The insertion of the RGD peptide at the HI-loop of the fiber allows CAR-independent target cell infection and increases virus infectivity.¹⁸ Moreover, genome sizes of Adwt-RGD and ICOVIR-15 are also indicated in the figure.

The palindromic E2F-binding sites in ICOVIR-15 enhance the antitumor activity of Adwt-RGD *in vitro* and *in vivo*

Due to deregulation of the retinoblastoma (Rb/p16) pathway, E2F is ubiquitously released from the E2F-Rb complexes in tumor cells.¹⁹ The binding of free E2F to E2F-palindromic sites in the *E1A* promoter of ICOVIR-15 should enhance the transcription of

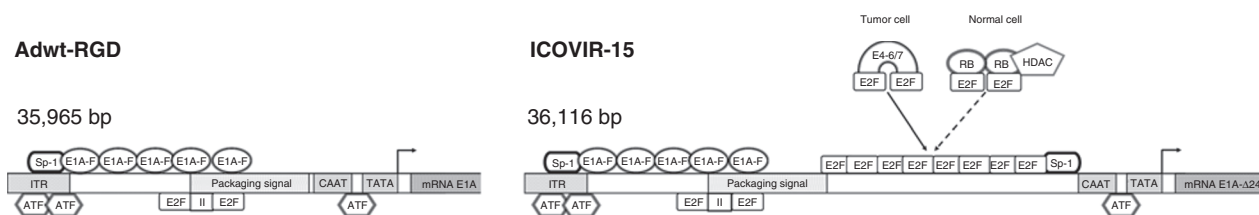


Figure 1 Schematic diagram of *E1A* transcriptional control. ICOVIR-15 incorporates eight extra E2F-responsive sites organized in four palindromes. Furthermore, one extra Sp-1-binding site was also inserted. Genetic modifications in ICOVIR-15 increase genome size by only 151 bp. In cancer cells, the E2F transcription factor is released from E2F-Rb complexes, due to pRb pathway deregulation. When ICOVIR-15 infects a tumor cell, free E2F binds to the E2F-palindrome sites present in the modified *E1A* promoter and activates E1A- Δ 24 transcription. The Sp-1 transcription factor cooperates with E2F to activate transcription. E1A proteins activate the transcription of the other early adenoviral proteins, including E4-6/7, which forms a complex with free E2F that binds to the palindromic E2F sites inserted in ICOVIR-15 promoter to further activate *E1A* transcription. The same palindromic E2F motif is also present in the *E2* promoter, resulting in an efficient loop of autoactivation and lysis of cancer cells. The RGD-modified fiber increases virus infectivity. In normal, quiescent cells, functional pRb forms an inhibitory complex with the E2F transcription factor. After infection of normal cells, binding of E2F-pRb complexes to the E2F-responsive sites inserted in ICOVIR-15 docks histone deacetylases to the *E1A* promoter and prevents E1A- Δ 24 transcription. Whereas the wt *E1A* protein can release free E2F from the pRb-E2F complexes, the Δ 24-deletion in *E1A* prevents this, thereby preventing an autoactivation loop driven by E2F in the event of leaky E1A- Δ 24 expression. Adwt-RGD, wild-type adenovirus with RGD-modified fiber; bp, base pair; HDAC, histone deacetylase; II, enhancer element II; ITR, inverted terminal repeat; RB, retinoblastoma protein.

the *E1A* gene. Higher levels of E1A proteins should enhance the transactivation of the other adenoviral early proteins, including E4-6/7. E4-6/7 protein forms a complex with two E2F transcription factors and induces the cooperative and stable binding of this complex to the palindromic E2F-binding site structure present in the *E2* promoter²⁰ and in the *E1A* promoter of ICOVIR-15,

activating a positive feedback that should culminate in higher production of virus progeny and lysis of the tumor cell. To confirm such hypothesis, a panel of tumor cell lines representing a wide range of cancer types was evaluated for the effects of ICOVIR-15 infection. As shown in **Figure 2a**, E1A protein levels after infection with ICOVIR-15 were higher than those after infection with

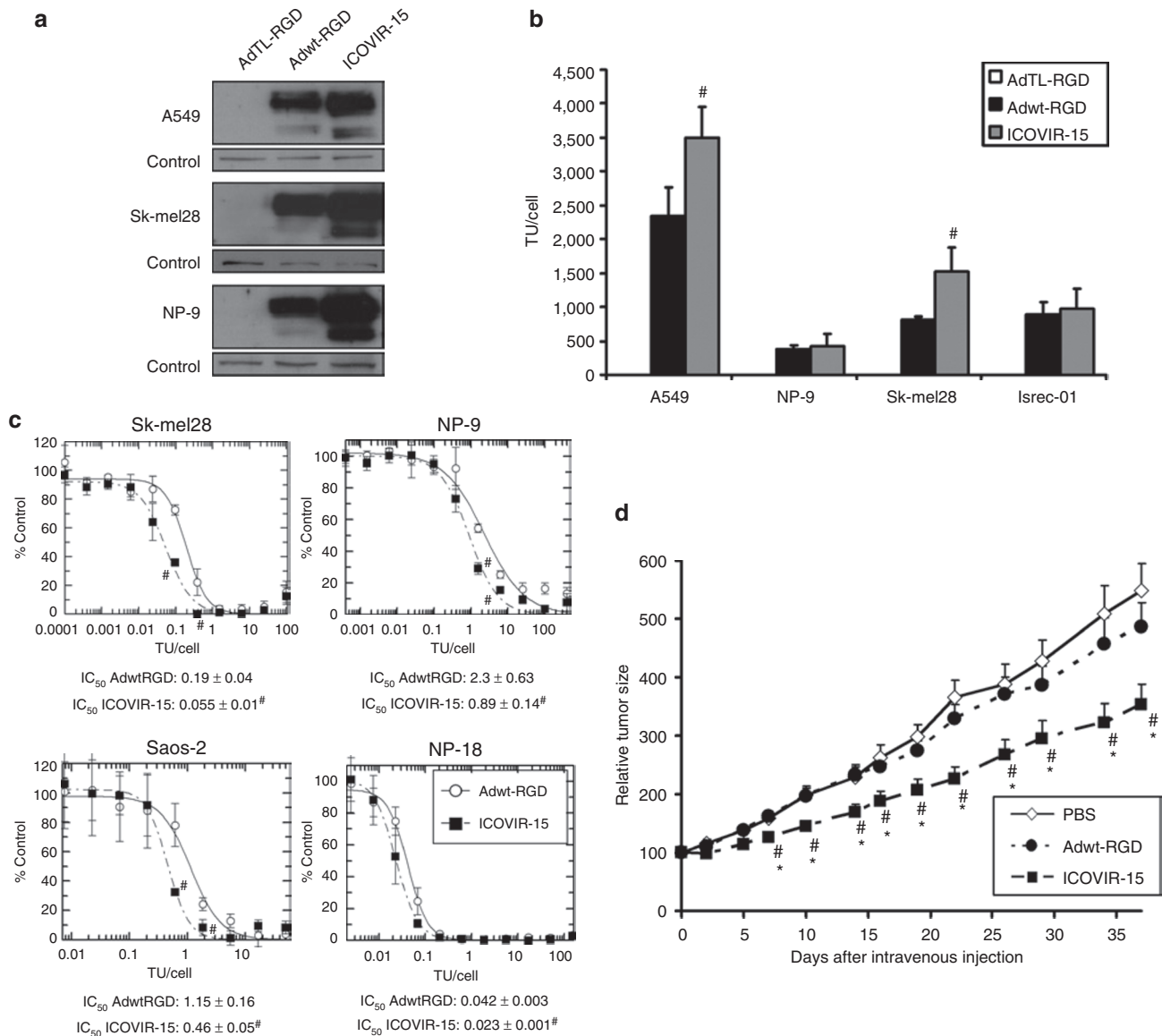


Figure 2 ICOVIR-15 improves antitumor efficacy compared to Adwt-RGD. **(a)** The E2F-responsive palindromes enhance the E1A expression driven by the endogenous *E1A* promoter. Anti-E1A western blots were performed 24 hours after infecting cells with a dose of each virus that allowed >80% transduction [multiplicity of infection (TU/cell) of 20 for Sk-mel28 and NP-9; 10 TU/cell for A549 cells]. The relative intensities of bands were measured by densitometry. AdTL-RGD is a replication-deficient control and Adwt-RGD is a wild-type adenovirus with an RGD-modified fiber. **(b)** Viral production of ICOVIR-15 in tumor cells. Different tumor cell lines were infected as indicated in **a** or with 20 transduction units (TU)/cell for Isrec-01. Virus production was measured 3 days after infection. Viral yield was evaluated in quadruplicate for each cell line, by carrying out two independent experiments. **(c)** Comparative cytotoxicity of ICOVIR-15. Cells were infected with the indicated viruses at doses ranging from 500 to 0.0001 TU/cell. IC₅₀ values (TU/cell required to cause a reduction of 50% in cell culture viability) at days 5–8 after infection are shown. Four different replicates were quantified for each cell line. Mean ± SD error bars are plotted. **(d)** Relative tumor growth after systemic injection of Adwt-RGD or ICOVIR-15. Nude mice harboring subcutaneous xenografts of Sk-mel28 cells (melanoma) were randomized and injected with a single intravenous dose of 2.5 × 10¹⁰ viral particles per mouse of Adwt-RGD or ICOVIR-15. Phosphate-buffered saline (PBS) administration was used as a control. ICOVIR-15 significantly reduced tumor growth compared to Adwt-RGD and PBS from early days in the experiment. Mean values of 16 tumors/group ± SE are depicted. #Significant *P* < 0.05 by two-tailed unpaired Student's *t*-test, compared to Adwt-RGD group. *Significant (*P* < 0.05) by two-tailed unpaired Student's *t*-test, compared to PBS group. Adwt-RGD, wild-type adenovirus with RGD-modified fiber.

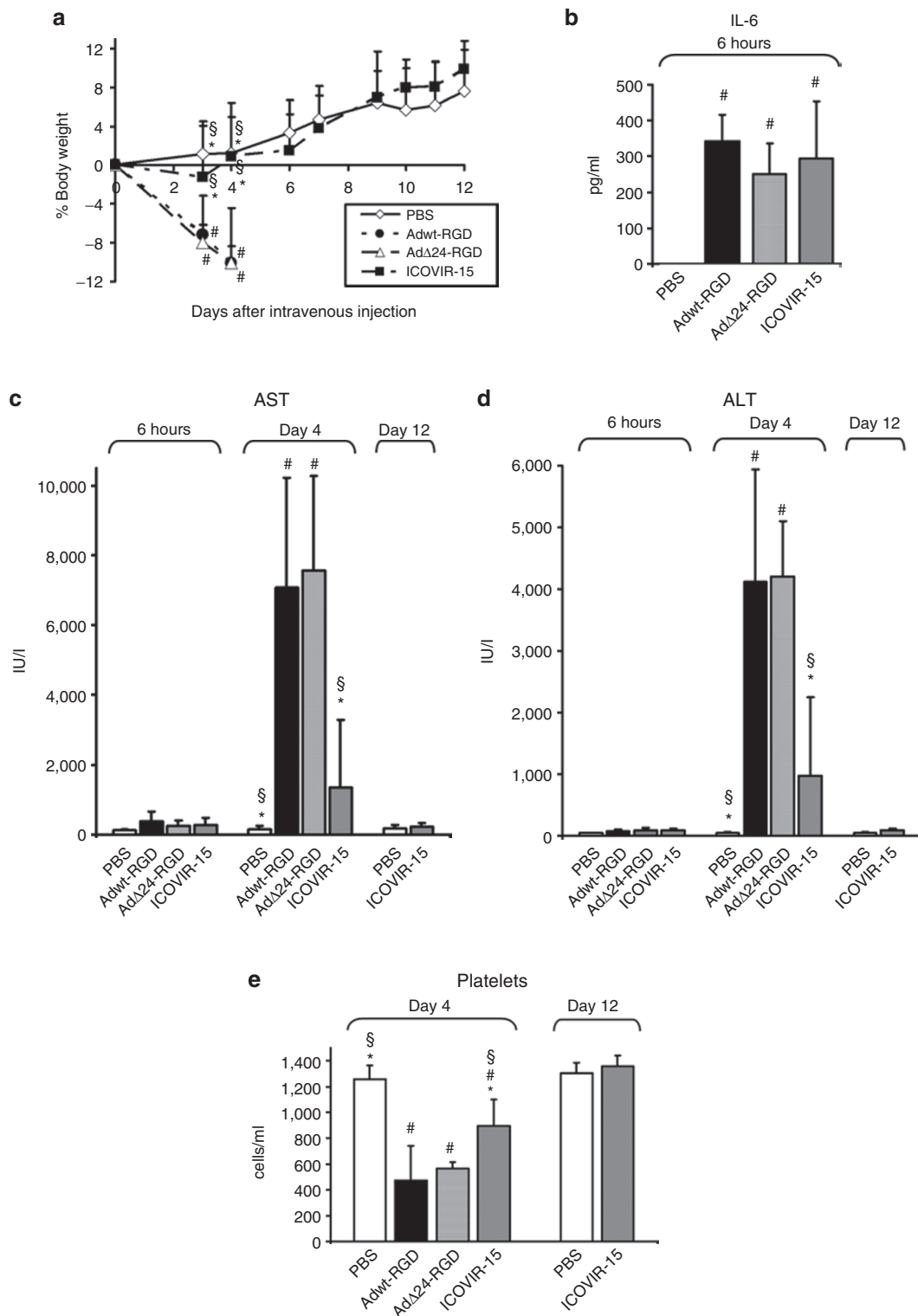


Figure 3 Toxicity profile after systemic injection of ICOVIR-15 in immunocompetent mice. **(a)** Body weight variation was monitored after intravenous administration of 5×10^{10} viral particles per mouse of Adwt-RGD, AdΔ24-RGD, or ICOVIR-15. Phosphate-buffered saline (PBS) administration was used in the control group. Adwt-RGD and AdΔ24-RGD-injected mice were killed at day 4 due to lethal toxicity, whereas ICOVIR-15-injected mice presented a similar weight profile than those injected with PBS. At 6 hours after administration, capsid-mediated IL-6 elevation was analyzed in **(b)** peripheral blood, meanwhile **(c,d)** serum transaminases and **(e)** platelet concentrations were analyzed at 6 hours, day 4 or day 12 after administration. Mean values \pm SD of 5–10 mice/group are depicted. *Significant ($P < 0.05$) by two-tailed unpaired Student's *t*-test, compared to Adwt-RGD group. §Significant ($P \leq 0.05$) by two-tailed unpaired Student's *t*-test, compared to AdΔ24-RGD group. #Significant ($P < 0.05$) by two-tailed unpaired Student's *t*-test, compared to PBS group. Adwt-RGD, wild-type adenovirus with RGD-modified fiber; ALT, alanine aminotransferase; AST, aspartate aminotransferase; IL-6, interleukin 6.

the parental virus Adwt-RGD in all cancer cell lines tested when analyzed by western blot and quantified by densitometry. E1A protein levels from ICOVIR-15 were 1.8, 3.4, and 4 times higher in A549, Sk-mel28, and NP-9, respectively, compared to Adwt-RGD levels.

To determine whether this increase in E1A amounts has a positive impact on the antitumoral potency, virus progeny production and cytotoxicity assays were performed. Virus progeny production was increased significantly for ICOVIR-15 in two out of four cancer cell lines tested, showing a trend for improvement in the other two (Figure 2b). When cytotoxicity was analyzed at days 5–8, the improvement became more evident because more than one cycle of replication occurred (Figure 2c). The E2F-binding sites rendered ICOVIR-15 more cytotoxic because the amount of virus required to reduce the cell culture viability by 50% (IC_{50}) was 3.5 times ($P \leq 0.022$), 2.5 times ($P \leq 0.017$), 2.5 times ($P \leq 0.007$), and 1.8 times ($P \leq 0.014$) lower in Sk-mel28, NP-9, Saos-2, and NP-18 cells, respectively, compared to the parental virus Adwt-RGD.

Once we had demonstrated the improved oncolytic potency of ICOVIR-15 *in vitro*, we tested whether this benefit is maintained in a tumor xenograft model. As disseminated disease is the most relevant clinical situation, systemic injection was used. Mice bearing Sk-mel28 (melanoma) tumors were injected with a single intravenous dose of phosphate-buffered saline (PBS), Adwt-RGD, or ICOVIR-15. The virus dose was 2.5×10^{10} viral particles per mouse, which is the maximum tolerated dose for systemic injection of wild-type adenoviruses in immunocompetent and nude mice.¹² ICOVIR-15 was more efficient at delaying the growth of Sk-mel28 subcutaneous tumors *in vivo* (Figure 2d). At day 37, when untreated mice had to be killed due to uncontrolled tumor growth, tumor size of Adwt-RGD-treated mice was 1.5-fold larger than in those treated with ICOVIR-15 ($P < 0.025$). Tumor size in PBS-treated mice was 1.8-fold larger than in the ICOVIR-15 group ($P < 0.005$).

In vivo systemic toxicity after ICOVIR-15 administration in Balb/C immunocompetent mice

Binding of pRb–E2F–HDAC complexes to E2F sites inserted into the *E1A* promoter should restrict transcription and diminish E1A-mediated toxicity in normal cells, thus allowing systemic administration for the treatment of disseminated neoplasias. The toxicity associated to a single intravenous dose of ICOVIR-15 or controls was assessed in Balb/C immunocompetent mice. Viruses were injected at a dose of 5×10^{10} viral particles per mouse and body weight was monitored daily. Adwt-RGD- and Ad Δ 24-RGD-injected mice were killed at day 4 after injection due to high decrease in body weight and high morbidity. In contrast, ICOVIR-15-injected group only suffered a 1% reduction in the body weight (not significant) at day 3 after administration and underwent a rapid recovery to PBS levels (Figure 3a).

Administration of adenoviruses induces two distinct peaks of inflammatory response.²¹ The early phase, occurring at 6 hours after administration, is capsid-mediated and has been associated with elevation of cytokines such as IL-6 (ref. 22). Adwt-RGD, Ad Δ 24-RGD, and ICOVIR-15 share identical capsids, and, accordingly, similar IL-6 concentrations in peripheral blood

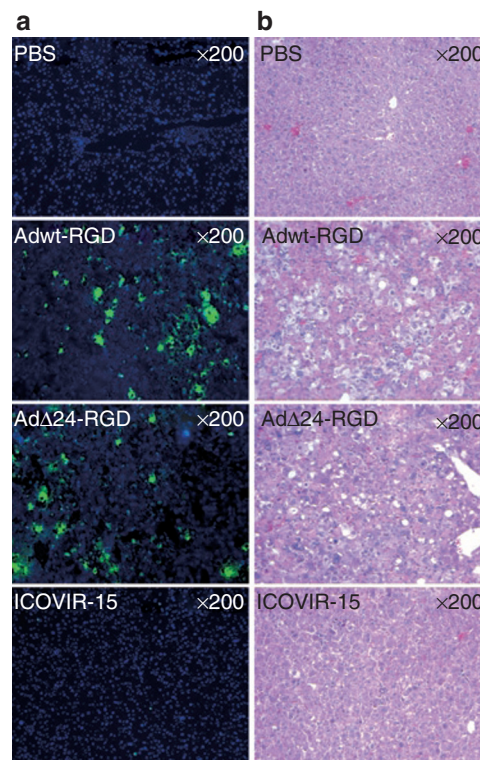


Figure 4 ICOVIR-15 reduces hepatic E1A expression *in vivo*. (a) Mouse livers were collected at day 4 after intravenous administration of PBS or viruses, and E1A expression was assessed by immunohistochemistry in frozen sections. E1A was barely detected in livers from mice injected with ICOVIR-15, whereas intense detection was observed throughout the livers of Adwt-RGD-injected mice. (b) E1A detection correlated with evident signs of hepatitis when analyzed by eosin–hematoxylin staining of paraffin-embedded liver sections. Pathological changes including macrosteatosis, presence of Councilman bodies, and large necrotic areas were present in livers from mice injected with Adwt-RGD, but not in those injected with ICOVIR-15. Adwt-RGD, wild-type adenovirus with RGD-modified fiber; PBS, phosphate-buffered saline.

were detected 6 hours after systemic administration (Figure 3b). Furthermore, as a large proportion of the oncolytic agent ends up in the liver after systemic administration, transaminase elevation has been reported in clinical trials after injections of high doses.² When transaminase enzymes (aspartate aminotransferase and alanine aminotransferase) were analyzed 6 hours after administration, only a slight nonsignificant increase was detected for both transaminases (Figure 3c,d). On the other hand, the second toxicity peak is dependent on transcription of viral proteins and it occurs at days 4–5 after administration. Up to a 44- and 87-fold elevation of aspartate aminotransferase and alanine aminotransferase, respectively, was detected in Adwt-RGD and Ad Δ 24-RGD-treated mice compared with nontreated animals when analyzed at day 4 after injection (Figure 3c,d). On the contrary, only a slight, transient transaminase elevation was detected in the ICOVIR-15-injected group. At day 4 after administration, an eightfold elevation in aspartate aminotransferase (not significant) and a 20-fold in alanine aminotransferase (not significant) were detected, but these elevations resolved by day 12. Furthermore, liver toxicity causes an increment in portal vein hypertension, the sequestration of platelets in the spleen and, consequently, a drop in platelet

count.²³ Although a serious thrombocytopenia was observed after Adwt-RGD or Ad Δ 24-RGD injection (2.6-fold reduction, $P \leq 0.002$), platelet depletion mediated by ICOVIR-15 was only 1.4-fold at day 4 and absent at day 12 (Figure 3d).

In addition, *E1A* expression was evaluated in murine liver sections by immunostaining as it is the main cause of toxicity in mice.⁹ Strong *E1A* staining was detected throughout livers from Adwt-RGD- and Ad Δ 24-RGD-injected mice (Figure 4a). On the contrary, little *E1A* was detected in livers from mice treated with ICOVIR-15 and this correlates with a histological analysis of liver sections (Figure 4b). Although evident symptoms of degenerative cirrhosis (macrosteatosis, presence of Councilman bodies, and large necrotic areas) were detected in livers from the Adwt-RGD and Ad Δ 24-RGD group, livers from ICOVIR-15-treated mice displayed an almost normal phenotype, with only marginal Councilman bodies in the superficial areas. These data indicate that the E2F-responsive palindromes inserted to control *E1A* expression are actively repressing transcription in normal cells. Once we confirmed that the dose of 5×10^{10} viral particles of ICOVIR-15 per mouse was well tolerated, we evaluated the systemic antitumoral activity of this novel oncolytic agent at this dose in several tumor xenograft models.

ICOVIR-15 exhibits potent antitumor efficacy and prolongs mouse survival after systemic administration

A549 (lung), NP-9 and NP-18 (pancreatic adenocarcinoma), PC-3 (prostate), and Sk-mel28 (melanoma) were selected as subcutaneous models in order to represent a range of tumor types. Mice carrying tumors were injected with a single intravenous dose of ICOVIR-15 at 5×10^{10} viral particles per mouse or PBS. When untreated animals displayed uncontrolled tumor growth, mice were killed. At killing, ICOVIR-15 treatment induced a reduction of more than 3.7-fold ($P < 0.0012$), threefold ($P < 0.012$), 2.3-fold ($P < 0.00007$), 2.8-fold ($P < 0.0001$), and 1.7-fold ($P < 0.03$) in the tumor size of NP-18, A459, Sk-mel28, NP-9, and PC-3 subcutaneous tumors, respectively (Figure 5a). Importantly, efficient tumor growth reduction was achieved in all subcutaneous tumor models tested. In addition, ICOVIR-15 treatment was able to significantly increase survival in all subcutaneous tumor models tested (Figure 5b).

The reduced genome size of ICOVIR-15 allows potent transgene expression without affecting viral kinetics

Late-phase expression of transgenes that promote viral spread or have cytotoxic effects may improve the ability of oncolytic adenovirus to eradicate tumors.¹ It is preferable to restrict transgene expression to the late phase of the virus replication cycle in order to minimize any antagonism between transgene activity and virus replication.²⁴ However, the ability of Ad5 to carry exogenous DNA is limited by its encapsidation capacity, which is ~ 38 kilobases.⁷ To determine whether the ICOVIR-15 backbone could be compatible with late transgene expression, we cloned the *NfsA* nitroreductase gene downstream of the fiber (Figure 6a). *Escherichia coli* nitroreductases, such as *NfsA* or *NfsB*, are flavoenzymes that can catalyze the reduction of nitro groups in a wide range of substrates, and they have been identified as useful in the metabolism of a number of prodrugs in anticancer gene therapy.²⁵ The *NfsA* gene cloned included the 3VDE splicing acceptor (IIIa virus

infection-dependent splicing enhancer) and a polyA sequence in order to promote its expression during the late phase of the viral life cycle.

To establish whether the insertion of *NfsA* alters virus replication, we compared virus progeny production and release of ICOVIR-15 and ICOVIR-15-*NfsA*. A549 cells were infected at high multiplicity of infection, and the amount of virus produced and released was determined at different time points. As shown in Figure 6b, the production and release kinetics of both viruses were similar at every time point, indicating that the transgene is not reducing the oncolytic potency of ICOVIR-15. Furthermore, the timing of nitroreductase expression was evaluated by western blot analysis to confirm late-phase expression. As shown in Figure 6c, *NfsA* was undetectable 24 hours after infection, its expression was slightly detected at 48 hours, and high amounts of transgene accumulated 72 hours after infection. To determine the functionality of *NfsA*, a cytotoxicity assay was performed in FaDu cells with or without CB1954 prodrug. When CB1954 was not present in the media, the amount of ICOVIR-15-*NfsA* required to reduce the cell culture viability by 50% (IC_{50}) was similar to that of ICOVIR-15 (Figure 6d). On the contrary, when a dose of 100 $\mu\text{mol/l}$ of CB1954 was added to the media, ICOVIR-15-*NfsA* IC_{50} was reduced five times ($P \leq 0.014$) compared with ICOVIR-15, indicating that *NfsA* is reducing CB1954 to toxic metabolites with bystander effect.

In summary, these results indicate that the new E2F-binding sites introduced into the *E1A* promoter in ICOVIR-15 are able to increase the antitumor potency of the wild-type adenovirus while drastically reducing toxicity after systemic injection. Moreover, its constrained genome size permits the insertion of transgenes without affecting the oncolytic potency.

DISCUSSION

Oncolytic adenoviruses have proven efficacious and relatively safe in the clinics.² However, clinical response rates are suboptimal, and further research is needed to improve the antitumor potency of these agents. One of the main limitations for efficacy is the inability of oncolytic adenoviruses to spread sufficiently within solid tumors.⁵ Some strategies aiming to increase adenovirus spread include mutations in E1B-19K,²⁶ overexpression of the adenovirus death protein,²⁷ or c-terminal truncating mutations in the i-leader protein.²⁸ However, several side effects such as virus yield reduction²⁹ or partial loss of the E3 immunomodulatory functions³⁰ have been reported with these approaches. An alternative strategy aiming to increase virus spread within the tumor mass is the expression of transgenes from the adenovirus backbone, such as proteases to disrupt the extracellular matrix⁵ or enzymes that convert prodrugs to diffusible cytotoxins that provide bystander killing of surrounding cells.³¹ However, the insertion of transgenes into the adenovirus genome is limited by the encapsidation size and requires transgene compatibility with the adenovirus replication cycle.

For an effective therapy, systemic delivery of the oncolytic agent is preferred in the clinical setting as patients may have inaccessible tumors or tumors that are already metastatic at the time of detection.³ Our group has previously described ICOVIR-7, an oncolytic adenovirus showing antitumor efficacy in a wide range of subcutaneous tumor models after systemic administration, with

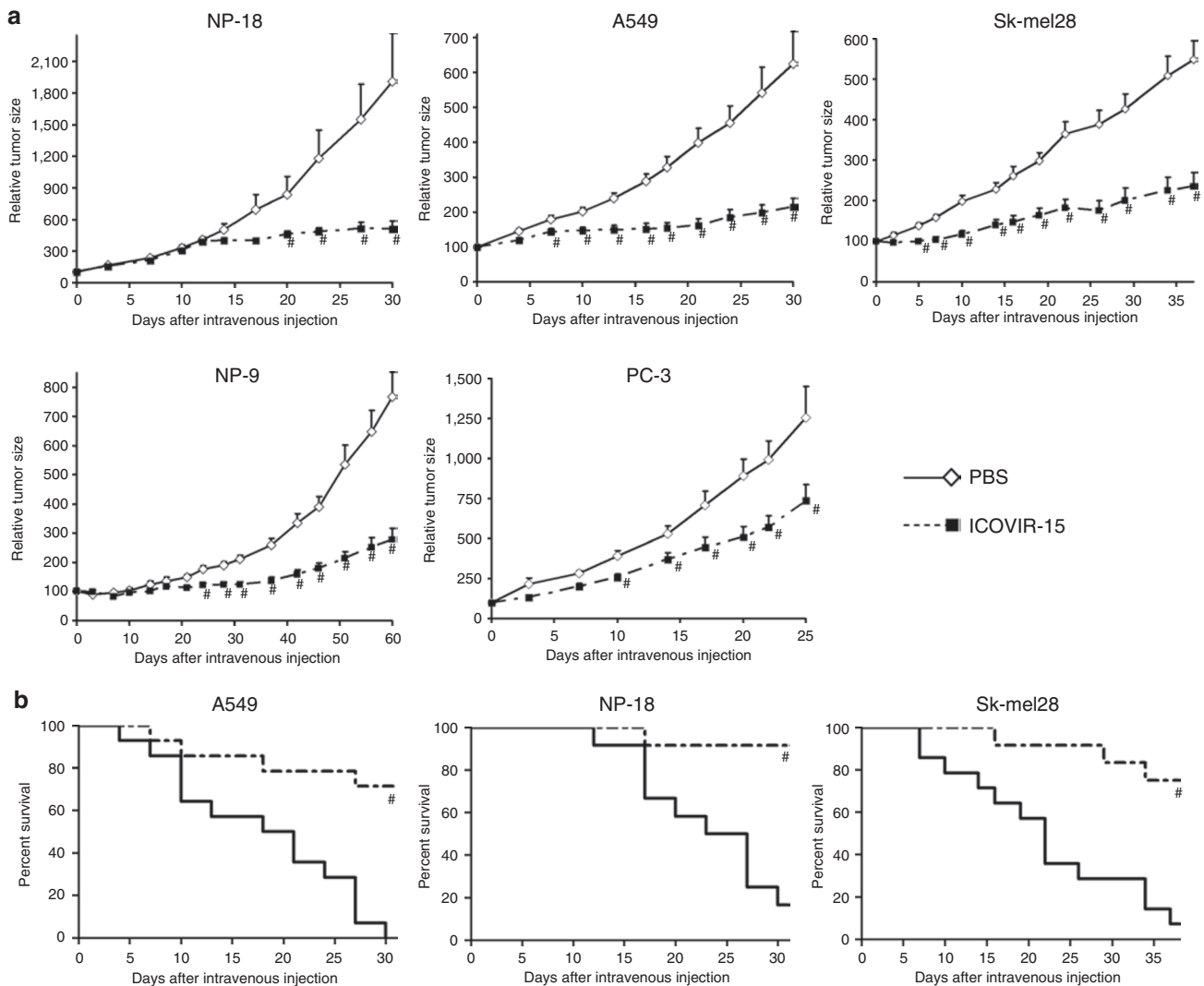


Figure 5 Efficacy and survival after systemic administration of ICOVIR-15. **(a)** Nude mice bearing subcutaneous xenografts of lung (A549), prostate (PC-3), pancreatic carcinoma (NP-9 and NP-18), or melanoma (Sk-mel28) were injected with a single intravenous dose of phosphate-buffered saline (PBS) or 5×10^{10} viral particles (vp) per mouse of ICOVIR-15. Relative tumor volume (percentages of size at treatment, mean \pm SE) of 12–18 tumors/group are plotted. #Significant $P < 0.05$ by two-tailed unpaired Student's t -test compared with mice injected with PBS. **(b)** Kaplan-Meier survival curves after administration of a single intravenous dose of PBS or 5×10^{10} vp per mouse of ICOVIR-15. The endpoint was established at a tumor volume of $\geq 500 \text{ mm}^3$. #Significant $P < 0.05$ by log-rank test compared with mice injected with PBS. PBS, phosphate-buffered saline.

a low toxicity profile.¹⁴ ICOVIR-7 controls the transcription of the E1A- $\Delta 24$ protein via an improved E2F-1 promoter insulated with the myotonic dystrophy locus insulator. It also contains an RGD-modified fiber to increase virus infectivity. Due to the benefits that the expression of certain transgenes may grant in terms of oncolytic potency, we considered arming this virus. However, the combination of all the genetic elements present in ICOVIR-7 raised its genome size to 37,053 bp, close to the 105% packaging limit,⁷ and when we attempted to introduce transgenes into this backbone, it resulted in genome instability and packaging problems (data not shown). As a measure to gain DNA insertion capacity, we deleted ORF 1 and 2, or ORF 1, 2, and 3 of the adenovirus E4 region. Although no important functions in replication have been associated with these proteins,³² the resulting viruses showed significant loss of potency and replication defects in cancer cells compared with their controls (S. Guedan, unpublished results).

Thus, we sought a novel modification that restricted a potent *E1A* transcription to cancer cells with only minimal increase in genome size, in order to retain the potential for efficient delivery and expression of additional transgenes.

Deregulation of the retinoblastoma (Rb/p16) pathway is a hallmark of tumor cells.³³ As a consequence of Rb pathway defects, E2F transcription factors are released, allowing activation of promoters containing E2F sites. Furthermore, the same E2F-binding sites can mediate silencing of these promoters in quiescent cells due to the formation of a complex involving E2F-pRb complexes and histone deacetylases.³⁴ An oncolytic adenovirus that controls E1A transcription by E2F sites may acquire potent, tumor-selective replication in a wide range of cancer cells. Importantly, a palindromic E2F-binding site pattern was described to perform an important role in adenovirus life cycle: the E4-6/7 protein forms a complex with two E2F transcription factors and induces

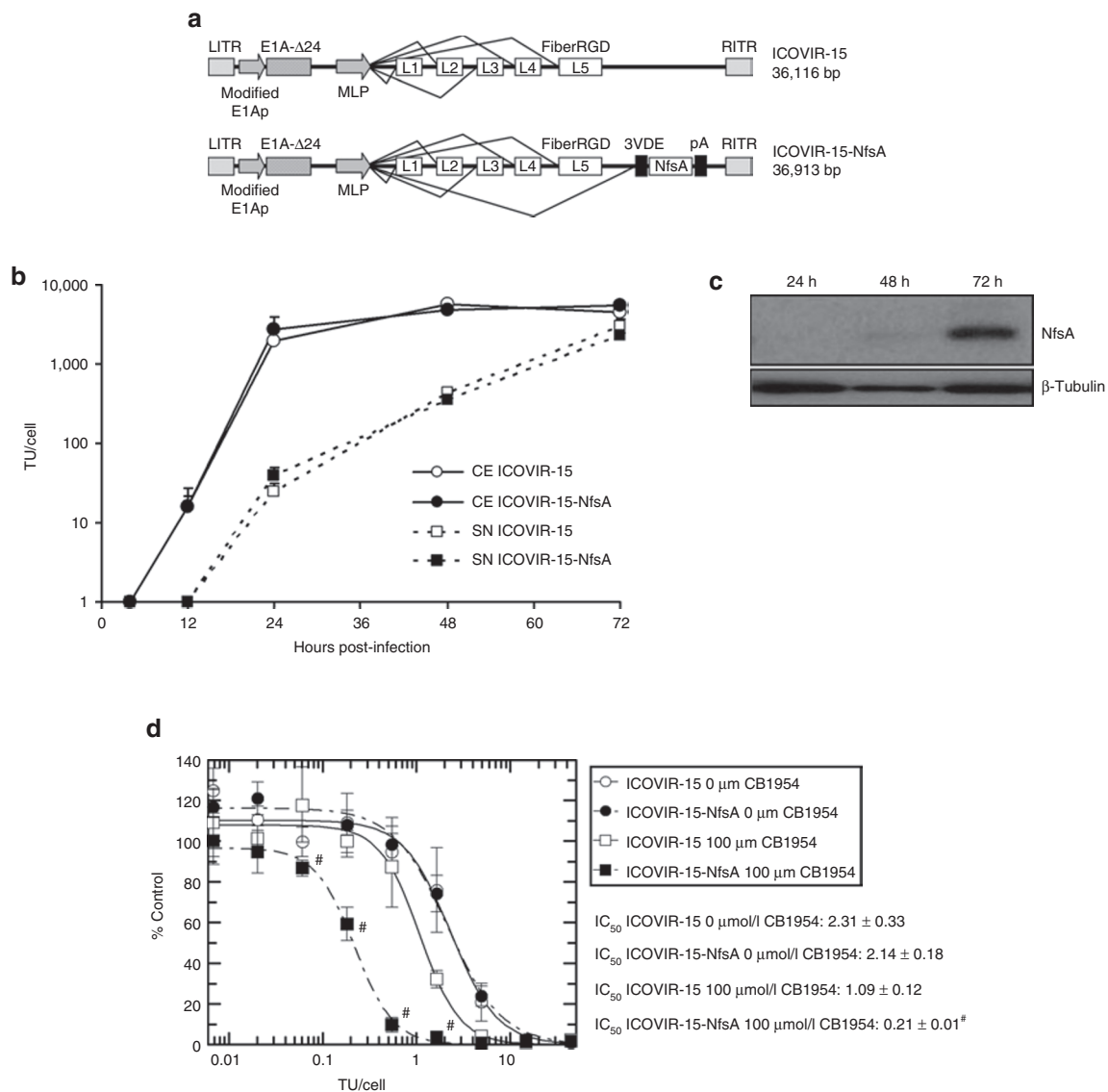


Figure 6 ICOVIR-15 is able to efficiently express transgenes. **(a)** Schematic representation of the genetic components present in ICOVIR-15 and ICOVIR-15-NfsA. To drive NfsA expression in ICOVIR-15-NfsA from the MLP, the Ad5 IIIa protein splice acceptor (3VDE) was inserted in front of the NfsA cDNA, followed by a polyA sequence (pA). These three elements were inserted downstream of the fiber-RGD in the ICOVIR-15 genome. The total lengths of both genomes are depicted in the figure. **(b)** Virus yield and release after infection with ICOVIR-15 and ICOVIR-15-NfsA. Confluent A549 cells were infected with 10 transduction units (TU)/cell. Four hours after infection, the viral solution was removed, and cell cultures were washed thrice with PBS and incubated with 1 ml of fresh virus-free medium. Cell extracts and supernatants were harvested 4, 12, 24, 48, and 72 hours after infection and titrated by an antihexon staining-based method. Viral yield and release were evaluated in quadruplicate. Mean \pm SD error bars are plotted. **(c)** Transgene expression driven by ICOVIR-15-NfsA. Anti-NfsA western blots were performed at the indicated time points after infection of PC-3 cells at a multiplicity of infection that allowed high transduction. β -Tubulin staining was used as loading control. **(d)** Comparative cytotoxicity of ICOVIR-15 and ICOVIR-15-NfsA in FaDu cells with and without CB1954 prodrug. FaDu cells were infected with the indicated viruses at doses ranging from 100 to 0.001 TU/cell. CB1954 was added at 100 μ mol/l to demonstrate NfsA activity. IC₅₀ values (TU/cell required to cause a reduction of 50% in cell culture viability) at day 6 after infection are shown. Four different replicates were quantified for each cell line. Mean \pm SD error bars are plotted. [#]Significant $P \leq 0.02$ by two-tailed unpaired Student's *t*-test compared with ICOVIR-15 plus CB1954 at 100 μ mol/l. 3VDE, IIIa virus infection-dependent splicing enhancer; CB1954, 5-(1-Aziridinyl)-2,4-dinitrobenzamide, 5-(Aziridin-1-yl)-2,4-dinitrobenzamide; CE, cell extract; MLP, major late promoter; pA, polyA sequence; SN, supernatant; TU, transduction units.

the cooperative and stable binding of E2F to this palindromic pattern to activate transcription.²⁰ This pattern is present in the *E2F-1* cellular promoter¹⁶ as S-phase induction is a requisite for the adenoviral life cycle. Moreover, this pattern is also present in the adenovirus type 5 *E2A* promoter to boost its transcription in response to E1A and E4 activation.³⁵ The presence of this pattern in the adenoviral genome suggests an optimal structure in terms

of DNA length to confer efficient E2F-responsiveness. Thus, we decided to construct a novel oncolytic adenovirus that contained palindromic E2F-binding sites in the *E1A* promoter. ICOVIR-15 incorporates eight new E2F-binding sites organized as four imperfect palindromes downstream of the packaging signal (Figure 1). Downstream of these palindromic sites, we also inserted one Sp-1-binding site, as Sp-1 was reported to play an important role

in the E2F-controlled promoters by interacting and cooperating to activate transcription.¹⁷ Contrary to an insulated exogenous promoter, this modification preserves the function of the element II in the *E1A* enhancer, which was previously reported to activate transcription of all of the early promoters in *cis*.³⁶ Moreover, as a measure to prevent an autoactivation loop by E2F in the case of promoter leakage, the pRb-binding site of *E1A* was deleted ($\Delta 24$ deletion).³⁷ An RGD motif was also inserted at the HI-loop of the fiber to increase virus infectivity to cancer cells.¹⁸

Taking into consideration that the mouse is not permissive for human adenovirus replication, the main toxicity in mice is associated with *E1A* expression.⁹ The palindromic E2F-binding sites present in ICOVIR-15 may repress *E1A* transcription in quiescent cells due to binding of E2F-pRb-histone deacetylase complexes, which strengthen the association of nucleosomes with DNA.³⁴ The systemic administration of Adwt-RGD or Ad $\Delta 24$ -RGD at a dose of 5×10^{10} viral particles per mouse caused an increase in transaminases levels, degeneration of liver tissue, hematological alterations, and severe weight loss (Figures 3 and 4). In fact, this dose represents more than the LD₅₀ value in immunocompetent mice for adenoviruses controlling *E1A* under the wild-type promoter.¹² In contrast, the injection of ICOVIR-15 at the same dose only caused slight alterations in transaminases levels and in platelet concentration at day 4 (Figure 3). This toxicity was transient and a complete recovery was achieved 12 days after the treatment. Thus, we can conclude that the insertion of palindromic E2F sites drastically reduces the toxicity following systemic administration of wild-type human adenovirus to mice.

Furthermore, our results demonstrate that the novel palindromic E2F-binding sites enhance the antitumor activity compared to wild-type human adenovirus. In contrast to some reports in which reduced *E1A* expression had little effect on replication,^{38,39} an increased level of *E1A* led to an improved viral yield, and this resulted in improved cytotoxicity in a variety of cell types including melanoma, osteosarcoma, and pancreatic adenocarcinomas (Figure 2a–c). Importantly, oncolytic potency improved in all tumor cell lines tested, in contrast to our previously described viruses where the presence of an insulated *E1A* promoter may limit the capacity of *E1A* enhancers to activate the other viral proteins.^{12,14} The benefit of ICOVIR-15 in terms of oncolytic potency was confirmed *in vivo*, where a single intravenous injection significantly increased the tumor growth inhibition relative to Adwt-RGD (Figure 2d). This experiment was performed at the maximum tolerated dose for Adwt-RGD by systemic injection in immunocompetent and nude mice. As ICOVIR-15 has lower toxicity than this nonselective virus and allows systemic injection at higher doses, the antitumor activity of a dose of 5×10^{10} viral particles per mouse was tested in a wide range of subcutaneous xenograft tumors, including melanoma, prostate, lung and pancreatic adenocarcinoma. A substantial benefit in the control of tumor growth and a significant increase in survival were observed compared to nontreated animals (Figure 5), suggesting an important antitumor activity of ICOVIR-15 when injected systemically.

As previously reported,⁴⁰ a histology analysis of tumors after adenovirus administration revealed that the presence of tumor stroma limits the complete intratumoral spread of the oncolytic agent (data not shown). This was especially noteworthy in the

PC-3 xenograft model, which expresses high amounts of matrix components.⁴¹ The expression of transgenes that contribute to disruption of the stromal barriers, such as proteolytic enzymes to degrade the matrix components⁴² or prodrug-converting enzymes to kill fibroblasts,³¹ may be used to enhance the viral spread within the tumor. Importantly, ICOVIR-15 has a similar genome size to wild-type adenovirus (only 150 bp more), which may facilitate the incorporation of transgenes. In order to evaluate whether the insertion of a transgene has negative effects on ICOVIR-15 replication, we constructed an armed version that incorporates an expression cassette of the transgene *NfsA*. *NfsA* is the major *Escherichia coli* nitroreductase and it can activate a variety of nitroaromatic prodrugs for cancer gene therapy.²⁵ The replication, the release, and the cytotoxicity of ICOVIR-15-*NfsA* were indistinguishable from those of its unarmed control (Figure 6b,c), indicating the suitability of ICOVIR-15 for delivering additional transgenes. Furthermore, *NfsA* expressed from ICOVIR-15 backbone was active as it minimized the amount of virus necessary to cause a reduction of 50% in tumor cell culture viability after adding CB1954 prodrug to the media (Figure 6c). To maintain tumor-selective expression of the transgene, we inserted additional splicing signals within the major late transcription unit. This strategy confers *E1A*-dependent transcription and achieves efficient, regulated transgene expression with a small DNA sequence. The 3VDE sequence (IIIa virus infection-dependent splicing enhancer) from the adenoviral IIIa protein is a useful splicing signal for late transgene expression because it is subject to a strict regulation during virus infection.⁴³ As shown in Figure 6c, the expression of *NfsA* driven by the 3VDE sequence in ICOVIR-15-*NfsA* was strictly restricted to the late phase of the viral cycle.

In addition to transgenes that enhance cytotoxicity or adenoviral distribution within the tumor, other transgenes may enhance the antitumor activity of ICOVIR-15. The expression of transgenes that modulate the tumor microenvironment, such as murine endostatin to inhibit the process of angiogenesis or TIMP3 to inhibit the action of matrix metalloproteinases, may improve the oncolysis by hindering tumor development.^{44,45} Furthermore, the expression of fusogenic proteins, such as GALV protein, may also enhance antitumor activity by syncytium formation.⁴³ On the other hand, a different strategy is the expression of factors that recruit immune cells to the site of infection and induce their proliferation and activation. This strategy has the potential to destroy not only the primary tumor, but also remote metastases. Cytokines, such as GM-CSF or MCP-3, or interleukins, such as IL-4 or IL-24, have been used previously to arm oncolytic adenoviruses.⁶ All these strategies would confer different characteristics to ICOVIR-15 and warrant testing as candidates for clinical trials.

In summary, our results indicate that ICOVIR-15 displays an appealing efficacy to toxicity ratio. On one hand, the inserted palindromic E2F-binding sites reduce the toxicity caused by systemic injection of adenoviruses. On the other hand, the same binding sites enhance the oncolytic potency even when compared to the nonselective wild-type adenovirus, which is particularly noteworthy due to the requirements of enhanced potency in the clinics. Importantly, the broad spectrum and the small genome size of this novel oncolytic adenovirus represent an optimal backbone to insert transgenes without deleting viral functions, which may help

to overcome the barriers imposed by the complex architecture of tumors.

MATERIALS AND METHODS

Cell culture. HEK293 (human embryonic kidney cells), A549 (human lung adenocarcinoma), Sk-mel28 (melanoma), PC-3 (prostate adenocarcinoma), Saos-2 (osteosarcoma), and FaDu (squamous cell carcinoma) cell lines were obtained from the American Type Culture Collection (Manassas, VA). NP-9 and NP-18 (pancreatic adenocarcinomas) cell lines were established in our laboratory.⁴⁶ Isrec-01 (colon cancer cell line) was a kind gift from R. Iggo (Institut Bergonié, Bordeaux, France). All tumor cell lines, excluding Isrec-01, were maintained in Dulbecco's modified Eagle's medium containing 5% fetal bovine serum at 37°C, 5% CO₂. Isrec-01 cells' Dulbecco's modified Eagle's medium was supplemented with 10% fetal bovine serum.

Viruses. Adwt-RGD, AdΔ24-RGD, and AdTL-RGD have been previously described.^{18,47,48} Adwt-RGD was propagated in A549 cells, and the replication-deficient AdTL-RGD and Ad-CMV-NfsA were propagated in HEK293 cells. ICOVIR-15 was created by inserting four E2F-binding site hairpins and one Sp-1-binding site following nucleotide 415 in the E1a promoter of AdΔ24-RGD.⁴⁷ To achieve this, a unique *Bsi*WI site was created by site-directed mutagenesis in the adenoviral shuttle vector pEndK/SpeI. An Sp-1 site was introduced using this plasmid digested with *Bsi*WI and the annealed oligonucleotides Sp1F (5'-GTACGTCGACCACAAAC CCCGCCAGCGTCTTGTCATTGGCGTCGACGCT-3') and Sp1R (5'-GTACAGCGTCGACGCCAATGACAAGACGCTGGGCGGGGTTTGTGGTCGAC-3'). E2F hairpins were introduced using the annealed oligonucleotides E2FF2 (5'-GTACGTCGCGGCTCGTGGCTCTTTCGCGGCAAAAAGGATTTGGCGCGTAAAAGTGGTTCGAA-3') and E2FR2 (5'-GTACTTCGAACCACTTTTACGCGCCAAATCCTTTTTGCGCGGAAAGAGCCACGAGCCGCCGAC-3') to create pEndKbsi415Sp1E2F2. For homologous recombination in yeast, the yeast replication elements and a selectable marker (CAU fragment⁴⁹) were cloned into this vector. The pEndKbsi415Sp1E2F2CAU linearized with *Kpn*I was recombined with AdΔ24-RGD genomic DNA in *Saccharomyces cerevisiae* YPH857 to construct pICOVIR-15. ICOVIR-15 was obtained by transfection into HEK293 cells of the large *Pac*I fragment of pICOVIR-15. ICOVIR-15-NfsA was constructed taking advantage of an *Spe*I site present in pAdwt-GALV-CAU, a replication-competent adenovirus previously described by us.⁴³ By homologous recombination in yeast, the E2F and Sp-1 sites, as well as the Δ24 mutation, were introduced. To clone the NfsA gene downstream of the fiber protein, plasmid pPS1374J1 was created by amplifying the NfsA from the pSV035 plasmid²⁵ using oligonucleotides 5'-CGTCAATTGTACTAAGCGGTGATGTTTCTGATCAGCCACCATGACGCCAACCATTG-3' and 5'-CAGCAATTGAAAATAAAGTTTATTAGCGCGTCCGCCAACCTG-3' and cloning the *Mfe*I-digested PCR product into the *Mfe*I site of pNK-FiberRGD.^{43,50} The pICOVIR-15-NfsA plasmid, containing the complete ICOVIR-15-NfsA genome, was created by homologous recombination in yeast between pPS1374J1, digested with *Kpn*I and *Not*I, and the pAdwt-GALV-CAU with E2F and Sp-1 sites, digested with *Spe*I. ICOVIR-15-NfsA was obtained by transfection in HEK293 cells of the *Pac*I fragment of pICOVIR-15-NfsA. Viruses were plaque-purified, amplified in A549 cells and purified using a CsCl gradient. Viral genomes were verified by restriction analysis and by sequencing E1A promoter, E1A-Δ24, RGD-modified fiber, and nitroreductase NfsA using oligonucleotides oligo22 (5'-AAGTGTGATGTTGCAAGTGT-3'), Ad670F (5'-ATCTTCCACCTCCTAGCCAT-3'), FiberUp (5'-CAAACGC TGTGGATTTATG-3'), and FiberDown2 (5'-GGCTATACTACTGAA TGAA-3').

Protein expression analysis. Cell cultures seeded in 24-well plates were infected at a multiplicity of infection that allowed at least 80% infectivity [20 transduction units (TU)/cell for Sk-mel28, NP-9, and PC-3, and

10¹⁰ TU/cell for A549 cells]. Whole-cell protein extracts were prepared at the indicated time after infection by incubation in lysis buffer (400 mmol/l NaCl, 1 mmol/l EDTA, 5 mmol/l NaF, 10% glycerol, 1 mmol/l sodium orthovanadate, 0.5% Nonidet NP-40, and a mixture of protease inhibitors (Sigma-Aldrich, St Louis, MO) in 10 mmol/l Tris-HCl pH 7.4) for 1 hour at 4°C. Clarified samples (15 μg/lane) were separated by a 10% SDS-PAGE gel and transferred to a nitrocellulose membrane (GE Healthcare, Arlington Heights, IL). For E1A protein, detection was performed by immunoblotting membranes using a polyclonal anti-E1A primary antibody (Rabbit, Clone 13S-5) (Santa Cruz Biotechnology, Santa Cruz, CA) and a polyclonal anti-rabbit conjugated with horseradish peroxidase (Goat; DakoCytomation, Carpinteria, CA). E1A bands from western blot were quantified using Bio-Rad GS-800 densitometer (Bio-Rad, Hercules, CA) and normalized using unspecific bands detected by the anti-E1A primary antibody. For NfsA detection, membranes were immunoblotted using a sheep anti-NfsA serum obtained from Alta Bioscience (Birmingham, UK), using purified NfsA protein kindly provided by E. Hyde and D. Jarrom (School of Biosciences, University of Birmingham, Birmingham, UK), and peroxidase-conjugated donkey anti-sheep secondary antibody (Sigma-Aldrich). A mouse monoclonal anti-β-tubulin antibody and a peroxidase-conjugated anti-mouse antibody (Goat; Sigma-Aldrich) were used for immunoblotting of β-tubulin as a loading control.

Virus release and production assays. Cell cultures (~2 × 10⁵ cells seeded in 24-well plates) were infected at a multiplicity of infection that allowed at least 80% infectivity (20 TU/cell for Sk-mel28, NP-9, and Isrec-01, and 10 TU/cell for A549 cells). Four hours after infection, cultures were washed thrice with PBS and incubated in fresh virus-free medium. At the indicated time points after infection, a small fraction of the supernatant was collected, and the cells and the medium were harvested and frozen-thawed three times to obtain the cell extract. Viral titers were determined by an antihexon staining-based method.¹²

In vitro cytotoxicity assays. Cytotoxicity assay was performed by seeding 20,000 NP-18 cells, 15,000 Saos-2, FaDu or NP-9 cells, or 10,000 Sk-mel28 per well in 96-well plates in Dulbecco's modified Eagle's medium with 5% fetal bovine serum. Cells were infected with serial dilutions starting with 800 TU/cell for NP-9 cells, 150 TU/cell for NP-18 or Saos-2 cells, or 100 TU/cell for Sk-mel28 or FaDu cells. For the nitroreductase activity assay, CB1954 (5-(1-Aziridinyl)-2,4-dinitrobenzamide, 5-(Aziridin-1-yl)-2,4-dinitrobenzamide, Sigma-Aldrich) at 100 μmol/l was added to the media at day 0. At days 5–8 after infection, plates were washed with PBS and stained for total protein content (bicinchoninic acid assay; Pierce Biotechnology, Rockford, IL). Absorbance was quantified, and the TU per cell required to produce 50% inhibition (IC50 value) was estimated from dose–response curves by standard nonlinear regression (GraFit; Erithacus Software, Horley, UK), using an adapted Hill equation.

In vivo toxicity study. Mice for toxicology and efficacy studies were maintained in the facility of the Institut de Recerca Oncològica-IDIBELL (Barcelona, Spain), AAALAC unit 1155. All animal studies have been approved by the Institut d'Investigació Biomèdica de Bellvitge Ethical Committee for Animal Experimentation. 5 × 10¹⁰ purified viral particles were injected intravenously into the tail vein in 6-week-old immunocompetent Balb/C male mice in a volume of 10 ml/kg in PBS (*n* = 5). Daily observations for body weight, morbidity, and moribundity were performed. At 6 hours, day 4 or day 12 after injection, mice were killed, and different samples were collected. Blood samples were collected by intracardiac puncture, and clinical biochemical and hematological determinations were performed by the Clinical Biochemistry and Hematological Services of the Veterinary Faculty at the Autonomous University of Barcelona. For IL-6 determination, we used a Basic Kit Mouse FlowCytomix complemented with Mouse IL-6 FlowCytomix (Bender MedSystems, Vienna, Austria), following manufacturer's instructions. The significance of differences in biochemical and hematological rates between treatment groups

was assessed by a two-tailed Student's unpaired *t*-test. Mice livers were resected and portions were fixed in 4% formaldehyde for 24 hours at room temperature (for paraffin embedding and further hematoxylin/eosin staining) or frozen in OCT (Sakura Finetek, Zoeterwoude, the Netherlands). E1A-immunodetection was performed by incubating OCT-embedded liver sections with a primary polyclonal antibody antiadenovirus-2 E1A (clone 13 S-5; Santa Cruz Biotechnology) and an AlexaFluor 488-labeled goat anti-rabbit antibody (Molecular Probes, Eugene, OR). Slides were counterstained with 4',6-diamino-2-phenylindole and visualized under a fluorescent microscope (Olympus BX51; Olympus Optical, Hamburg, Germany).

In vivo antitumoral efficacy. Subcutaneous A549, Sk-mel28, NP-9, NP-18, or PC-3 carcinoma tumors were established by injection of 1×10^7 cells into the flanks of 6-week-old male Balb/C *nu/nu* mice. When tumors reached 100 mm³ (experimental day 0), mice were randomized ($n = 10-16$ per group) and were injected by a single intravenous injection of PBS, 2.5×10^{10} viral particles of Adwt-RGD or ICOVIR-15, or 5×10^{10} viral particles of ICOVIR-15 in a volume of 10 ml/kg in PBS via the tail vein. Tumor size and mice status were monitored thrice per week. Tumor volume was defined by the equation $V \text{ (mm}^3\text{)} = \pi/6 \times W^2 \times L$, where *W* and *L* are the width and the length of the tumor, respectively. Data are expressed as relative tumor size at the beginning of the therapy, which was set as 100%. The significance of differences in relative tumor size between treatment groups was assessed by a two-tailed Student's unpaired *t*-test. For Kaplan–Meier survival curves, end point was established at $\geq 500 \text{ mm}^3$. The survival curves obtained were compared for the different treatments. Animals whose tumor size never achieved the threshold were included as right censored information. A log-rank test was used to determine the statistical significance of the differences in time-to-event.

ACKNOWLEDGMENTS

We thank Blanca Luena, Cristina Puig, Eduard Serra, and Liz Hodgkins for their technical assistance. J.J.R. and S.G. were supported by a predoctoral fellowship (FI) granted by the Generalitat de Catalunya. This work was supported by BIO2008-04692-C03-01 (R.A.) and FIS grant PI08/1661 (M.C.) from the Ministerio de Ciencia y Tecnología of the Government of Spain, by 2005-SGR-00727 from the Departament d'Universitats, Recerca i Societat de la Informació of the Generalitat de Catalunya (R.A.), by grant C1007/A6688 from Cancer Research UK (P.F.S.) and by the Birmingham Experimental Cancer Medicine Centre (award C1520, P.F.S.). R.A. belongs to the Network of Cooperative Research on Cancer (C03-10), Instituto de Salud Carlos III of the Ministerio de Sanidad y Consumo, Government of Spain. The authors declared no conflict of interest.

REFERENCES

- Aleman, R (2007). Cancer selective adenoviruses. *Mol Aspects Med* **28**: 42–58.
- Aghi, M and Martuza, RL (2005). Oncolytic viral therapies—the clinical experience. *Oncogene* **24**: 7802–7816.
- Nemunaitis, J, Cunningham, C, Buchanan, A, Blackburn, A, Edelman, G, Maples, P *et al.* (2001). Intravenous infusion of a replication-selective adenovirus (ONYX-015) in cancer patients: safety, feasibility and biological activity. *Gene Ther* **8**: 746–759.
- Parato, KA, Senger, D, Forsyth, PA and Bell, JC (2005). Recent progress in the battle between oncolytic viruses and tumours. *Nat Rev Cancer* **5**: 965–976.
- Kim, JH, Lee, YS, Kim, H, Huang, JH, Yoon, AR and Yun, CO (2006). Relaxin expression from tumor-targeting adenoviruses and its intratumoral spread, apoptosis induction, and efficacy. *J Natl Cancer Inst* **98**: 1482–1493.
- Cody, JJ and Douglas, JT (2009). Armed replicating adenoviruses for cancer virotherapy. *Cancer Gene Ther* **16**: 473–488.
- Bett, AJ, Prevec, L and Graham, FL (1993). Packaging capacity and stability of human adenovirus type 5 vectors. *J Virol* **67**: 5911–5921.
- Suzuki, K, Aleman, R, Yamamoto, M and Curiel, DT (2002). The presence of the adenovirus E3 region improves the oncolytic potency of conditionally replicative adenoviruses. *Clin Cancer Res* **8**: 3348–3359.
- Engler, H, Machemer, T, Philopena, J, Wen, SF, Quijano, E, Ramachandra, M *et al.* (2004). Acute hepatotoxicity of oncolytic adenoviruses in mouse models is associated with expression of wild-type E1a and induction of TNF- α . *Virology* **328**: 52–61.
- Rodriguez, R, Schuur, ER, Lim, HY, Henderson, GA, Simons, JW and Henderson, DR (1997). Prostate attenuated replication competent adenovirus (ARCA) CN706: a selective cytotoxic for prostate-specific antigen-positive prostate cancer cells. *Cancer Res* **57**: 2559–2563.
- Huch, M, Gros, A, José, A, González, JR, Alemany, R and Fillat, C (2009). Urokinase-type plasminogen activator receptor transcriptionally controlled adenoviruses eradicate pancreatic tumors and liver metastasis in mouse models. *Neoplasia* **11**: 518–528, 4 p following 528.
- Cascallo, M, Alonso, MM, Rojas, JJ, Perez-Gimenez, A, Fueyo, J and Alemany, R (2007). Systemic toxicity-efficacy profile of ICOVIR-5, a potent and selective oncolytic adenovirus based on the pRB pathway. *Mol Ther* **15**: 1607–1615.
- Taki, M, Kagawa, S, Nishizaki, M, Mizuguchi, H, Hayakawa, T, Kyo, S *et al.* (2005). Enhanced oncolysis by a tropism-modified telomerase-specific replication-selective adenoviral agent OBP-405 ('Telomelysin-RGD'). *Oncogene* **24**: 3130–3140.
- Rojas, JJ, Cascallo, M, Guedan, S, Gros, A, Martínez-Quintanilla, J, Hemminki, A *et al.* (2009). A modified E2F-1 promoter improves the efficacy to toxicity ratio of oncolytic adenoviruses. *Gene Ther* **16**: 1441–1451.
- Yoshida, K, Higashino, F and Fujinaga, K (1995). Transcriptional regulation of the adenovirus E1A gene. *Curr Top Microbiol Immunol* **199** (Pt 3): 113–130.
- Neuman, E, Flemington, EK, Sellers, WR and Kaelin, WG Jr (1994). Transcription of the E2F-1 gene is rendered cell cycle dependent by E2F DNA-binding sites within its promoter. *Mol Cell Biol* **14**: 6607–6615.
- Karseder, J, Rotheneder, H and Wintersberger, E (1996). Interaction of Sp1 with the growth- and cell cycle-regulated transcription factor E2F. *Mol Cell Biol* **16**: 1659–1667.
- Suzuki, K, Fueyo, J, Krasnykh, V, Reynolds, PN, Curiel, DT and Alemany, R (2001). A conditionally replicative adenovirus with enhanced infectivity shows improved oncolytic potency. *Clin Cancer Res* **7**: 120–126.
- Sherr, CJ and McCormick, F (2002). The RB and p53 pathways in cancer. *Cancer Cell* **2**: 103–112.
- Schaley, J, O'Connor, RJ, Taylor, LJ, Bar-Sagi, D and Hearing, P (2000). Induction of the cellular E2F-1 promoter by the adenovirus E4-6/7 protein. *J Virol* **74**: 2084–2093.
- Liu, Q, Zais, AK, Colarusso, P, Patel, K, Haljan, G, Wickham, TJ *et al.* (2003). The role of capsid-endothelial interactions in the innate immune response to adenovirus vectors. *Hum Gene Ther* **14**: 627–643.
- Kiang, A, Hartman, ZC, Everett, RS, Serra, D, Jiang, H, Frank, MM *et al.* (2006). Multiple innate inflammatory responses induced after systemic adenovirus vector delivery depend on a functional complement system. *Mol Ther* **14**: 588–598.
- Kodama, T, Takehara, T, Hikita, H, Shimizu, S, Li, W, Miyagi, T *et al.* (2010). Thrombocytopenia exacerbates cholestasis-induced liver fibrosis in mice. *Gastroenterology* **138**: 2487–2498, 2498.e1–e7.
- Lukashev, AN, Fuerer, C, Chen, MJ, Searle, P and Iggo, R (2005). Late expression of nitroreductase in an oncolytic adenovirus sensitizes colon cancer cells to the prodrug CB1954. *Hum Gene Ther* **16**: 1473–1483.
- Vass, SO, Jarrom, D, Wilson, WR, Hyde, E and Searle, PF (2009). E. coli NfsA: an alternative nitroreductase for prodrug activation gene therapy in combination with CB1954. *Br J Cancer* **100**: 1903–1911.
- Liu, TC, Hallden, G, Wang, Y, Brooks, G, Francis, J, Lemoine, N *et al.* (2004). An E1B-19 kDa gene deletion mutant adenovirus demonstrates tumor necrosis factor-enhanced cancer selectivity and enhanced oncolytic potency. *Mol Ther* **9**: 786–803.
- Toth, K, Djeha, H, Ying, B, Tollefson, AE, Kuppuswamy, M, Doronin, K *et al.* (2004). An oncolytic adenovirus vector combining enhanced cell-to-cell spreading, mediated by the ADP cytolytic protein, with selective replication in cancer cells with deregulated wnt signaling. *Cancer Res* **64**: 3638–3644.
- Subramanian, T, Vijayalingam, S and Chinnadurai, G (2006). Genetic identification of adenovirus type 5 genes that influence viral spread. *J Virol* **80**: 2000–2012.
- Pilder, S, Logan, J and Shenk, T (1984). Deletion of the gene encoding the adenovirus 5 early region 1b 21,000-molecular-weight polypeptide leads to degradation of viral and host cell DNA. *J Virol* **52**: 664–671.
- Wang, Y, Hallden, G, Hill, R, Anand, A, Liu, TC, Francis, J *et al.* (2003). E3 gene manipulations affect oncolytic adenovirus activity in immunocompetent tumor models. *Nat Biotechnol* **21**: 1328–1335.
- Chen, MJ, Green, NK, Reynolds, GM, Flavell, JR, Mautner, V, Kerr, DJ *et al.* (2004). Enhanced efficacy of Escherichia coli nitroreductase/CB1954 prodrug activation gene therapy using an E1B-55K-deleted oncolytic adenovirus vector. *Gene Ther* **11**: 1126–1136.
- Täuber, B and Dobner, T (2001). Molecular regulation and biological function of adenovirus early genes: the E4 ORFs. *Gene* **278**: 1–23.
- Sherr, CJ (2001). The INK4a/ARF network in tumour suppression. *Nat Rev Mol Cell Biol* **2**: 731–737.
- Black, AR and Azizkhan-Clifford, J (1999). Regulation of E2F: a family of transcription factors involved in proliferation control. *Gene* **237**: 281–302.
- Kovesdi, I, Reichel, R and Nevins, JR (1986). Identification of a cellular transcription factor involved in E1A trans-activation. *Cell* **45**: 219–228.
- Hearing, P and Shenk, T (1986). The adenovirus type 5 E1A enhancer contains two functionally distinct domains: one is specific for E1A and the other modulates all early units in cis. *Cell* **45**: 229–236.
- Fueyo, J, Gomez-Manzano, C, Aleman, R, Lee, PS, McDonnell, TJ, Mitlianga, P *et al.* (2000). A mutant oncolytic adenovirus targeting the Rb pathway produces anti-glioma effect *in vivo*. *Oncogene* **19**: 2–12.
- Hitt, MM and Graham, FL (1990). Adenovirus E1A under the control of heterologous promoters: wide variation in E1A expression levels has little effect on virus replication. *Virology* **179**: 667–678.
- Nettelbeck, DM, Rivera, AA, Balagué, C, Aleman, R and Curiel, DT (2002). Novel oncolytic adenoviruses targeted to melanoma: specific viral replication and cytotoxicity by expression of E1A mutants from the tyrosinase enhancer/promoter. *Cancer Res* **62**: 4663–4670.
- Georger, B, Vassal, G, Opolon, P, Dirven, CM, Morizet, J, Laudani, L *et al.* (2004). Oncolytic activity of p53-expressing conditionally replicative adenovirus AdDelta24-p53 against human malignant glioma. *Cancer Res* **64**: 5753–5759.

41. Ricciardelli, C, Russell, DL, Ween, MP, Mayne, K, Suwihat, S, Byers, S *et al.* (2007). Formation of hyaluronan- and versican-rich pericellular matrix by prostate cancer cells promotes cell motility. *J Biol Chem* **282**: 10814–10825.
42. Ganesh, S, Gonzalez Edick, M, Idamakanti, N, Abramova, M, Vanroey, M, Robinson, M *et al.* (2007). Relaxin-expressing, fiber chimeric oncolytic adenovirus prolongs survival of tumor-bearing mice. *Cancer Res* **67**: 4399–4407.
43. Guedan, S, Gros, A, Cascallo, M, Vile, R, Mercade, E and Alemany, R (2008). Syncytia formation affects the yield and cytotoxicity of an adenovirus expressing a fusogenic glycoprotein at a late stage of replication. *Gene Ther* **15**: 1240–1245.
44. Zhang, Q, Nie, M, Sham, J, Su, C, Xue, H, Chua, D *et al.* (2004). Effective gene-viral therapy for telomerase-positive cancers by selective replicative-competent adenovirus combining with endostatin gene. *Cancer Res* **64**: 5390–5397.
45. Lamfers, ML, Gianni, D, Tung, CH, Idema, S, Schagen, FH, Carette, JE *et al.* (2005). Tissue inhibitor of metalloproteinase-3 expression from an oncolytic adenovirus inhibits matrix metalloproteinase activity *in vivo* without affecting antitumor efficacy in malignant glioma. *Cancer Res* **65**: 9398–9405.
46. Villanueva, A, García, C, Paules, AB, Vicente, M, Megías, M, Reyes, G *et al.* (1998). Disruption of the antiproliferative TGF-beta signaling pathways in human pancreatic cancer cells. *Oncogene* **17**: 1969–1978.
47. Bauerschmitz, GJ, Lam, JT, Kanerva, A, Suzuki, K, Nettelbeck, DM, Dmitriev, I *et al.* (2002). Treatment of ovarian cancer with a tropism modified oncolytic adenovirus. *Cancer Res* **62**: 1266–1270.
48. Dmitriev, I, Krasnykh, V, Miller, CR, Wang, M, Kashentseva, E, Mikheeva, G *et al.* (1998). An adenovirus vector with genetically modified fibers demonstrates expanded tropism via utilization of a coxsackievirus and adenovirus receptor-independent cell entry mechanism. *J Virol* **72**: 9706–9713.
49. Sikorski, RS and Hieter, P (1989). A system of shuttle vectors and yeast host strains designed for efficient manipulation of DNA in *Saccharomyces cerevisiae*. *Genetics* **122**: 19–27.
50. Cascante, A, Abate-Daga, D, Garcia-Rodríguez, L, González, JR, Alemany, R and Fillat, C (2007). GCV modulates the antitumoural efficacy of a replicative adenovirus expressing the Tat8-TK as a late gene in a pancreatic tumour model. *Gene Ther* **14**: 1471–1480.